

Intergalactic globular clusters and the faint end of the galaxy number counts in A1656 (Coma)

A. Marín-Franch

Instituto de Astrofísica de Canarias, E-38205 La Laguna, Tenerife, Spain

amarin@ll.iac.es

and

A. Aparicio

Instituto de Astrofísica de Canarias, E-38205 La Laguna, Tenerife, Spain

aaaj@ll.iac.es

ABSTRACT

The existence of an intergalactic globular cluster population in the Coma cluster of galaxies has been tested using surface-brightness fluctuations. The main result is that the intergalactic globular cluster surface density (N_{IGC}) does not correlate with the distance to the center of Coma and hence with the environment. Furthermore, comparing these results with different Coma mass-distribution model predictions, it is suggested that N_{IGC} must in fact be zero all over Coma. On the other hand, the results for N_{IGC} and the faint end of the galaxy number counts (beyond $m_R = 23.5$) are connected. So $N_{\text{IGC}} = 0$ settles the slope of this function, which turns out to be $\gamma = 0.36 \pm 0.01$ down to $m_R = 26.5$.

The fact that $N_{\text{IGC}} = 0$ all over Coma suggests that globular clusters were formed only, or almost only, from protogalactic clouds. None, or perhaps very few, could have formed in isolated regions. It also seems inappropriate to advocate a relationship between intergalactic globular clusters and dark matter distributions, although it is true that the relationship could still exist but not be strong enough to have been detected. Finally, since our conclusion is that intergalactic globular clusters do not exist in Coma, accretion of intergalactic globular clusters might not be significant in galaxy formation and evolutionary processes in the Coma galaxies.

Subject headings: galaxies:clusters:individual (Coma)—galaxies:star clusters—galaxies:formation—galaxies:evolution—galaxies:luminosity function

1. Introduction

Intergalactic globular clusters (IGCs) are not bound to any particular galaxy but move freely in the potential wells of galaxy clusters. Table 1 will help the reader with the notation used in this paper. The existence of IGCs has been considered by a number of authors. The first discussion about them was by van den Bergh (1956), who measured the distance to the Abell No. 4 globular cluster (GC). Obtaining a distance modulus of 20.8, he concluded that it is therefore an *intergalactic tramp*. Van den Bergh (1958) estimated that the number of IGCs within the Local Group is one third of the total number of GCs. But the first real quantitative studies of IGCs in galaxy clusters were done by Forte, Martínez, & Muzzio (1982) and Muzzio (1987).

Muzzio (1987) suggested that galaxies in galaxy clusters suffer several dynamical effects owing to encounters with neighboring galaxies and to the action of the general galaxy cluster field; as a result, galaxies lose some GCs. Since these processes are very sensitive to the distribution of the total mass of the galaxy cluster, the study of IGCs may help us to solve the problem of how the *missing mass* is distributed. In this scenario, the number density of lost IGCs should follow the total mass distribution; hence, they might be concentrated toward the center of the galaxy cluster. In the same context, White (1987) suggested that cD envelopes and the diffuse light in Coma have the same origin: they are composed of stars tidally stripped from galaxies during Coma’s collapse. So GCs might have been stripped as well, creating an IGC population.

Alternatively, if IGCs do exist in galaxy clusters, they may have been formed in situ in scenarios such as biased GC formation. West (1993) argued that the number density of GCs in biased formation scenarios is extremely sensitive to the presence and amplitude of a background field, such as galaxy cluster-sized and galaxy-sized perturbations in the primordial matter distribution. GCs would have been much more likely to form in developing protogalaxies than in complete isolation, but a small number of IGCs is expected. In these scenarios, the number density of IGCs would be very small, and also might follow the galaxy cluster mass distribution.

From a galaxy formation point of view, as GCs are thought to be among the oldest objects in the Universe, they provide useful information about the galaxy formation and evolution processes. By studying a globular cluster system (GCS) associated with a single galaxy, the history of the host galaxy is probed. The hypothesis of the existence of an IGC population has been used to gain insight into the high- S_N problem. West et al. (1995) argued that a high value of S_N in galaxies located near the centers of galaxy clusters is the result of the accretion of a number of IGCs. They assumed that an IGC population exists in all galaxy clusters, and that the number density of IGCs is concentrated toward the center

of the galaxy cluster.

Recently, Côté et al. (2001) did a dynamical analysis of the GCS associated with M87. They concluded that the metal-rich GCs of M87 formed with the galaxy, and that the metal-poor GCs are gradually accreting onto M87 along Virgo’s principal axis. This could therefore be an example of how the accretion of IGCs would influence the galaxy’s evolutionary history.

Although some authors consider that the accretion of IGCs is capable of modifying the properties of the GCS of a galaxy, there are a number of others that defend the view that the greater part of a GCS is formed in situ from the protogalactic cloud (Blakeslee et al. 1997; Forbes, Brodie, & Grillmair 1997; Harris et al. 1998; McLaughlin 1999). So the possible influence of the accretion of IGCs in galaxy formation and evolutionary models is still an open issue. In this context, the existence or not of IGCs and, if they do exist, their abundance and distribution become crucial ingredients in the development of a unified galaxy evolution scenario.

Even though the existence of IGCs is often assumed, there is little evidence to date to prove this. Do GCs form only during starbursts in galaxies or can they form in isolation? If IGCs exist in all galaxy clusters, their number and spatial distribution are fundamental pieces of information for testing the different GC formation models. Furthermore, the influence of IGCs in the evolution of elliptical galaxies is still not clear. Is accretion of IGCs important during the galaxy’s formation and evolutionary history? If this is the case, is it important for all elliptical galaxies, or only for those located in some privileged locations inside galaxy clusters? In this paper the existence of an IGC population in the Coma galaxy cluster has been tested and quantified using the surface-brightness fluctuations (SBF) technique.

Our purpose is to obtain information about the IGC population from the study of the unresolved point sources by means of SBF analysis. The measured SBF signal is produced mainly by faint galaxies and the IGC population (if such a thing exists). For this reason, during SBF measurements, a good characterization of the faint end of the background differential galaxy number counts, $n(m)$, is fundamental. A number of authors have measured the slope of the faint end of $n(m)$ in the R filter. Results range from $\gamma = 0.39$ (Tyson 1988) to $\gamma = 0.31$ – 0.34 (Steidel & Hamilton 1993). This slope has also been measured in the Hubble Deep Field (Williams et al. 1996), with $\gamma = 0.36$ for the V filter and $\gamma = 0.31$ for the I filter down to magnitude 26. For the intermediate R filter, the slope must be between $\gamma = 0.31$ and 0.36 . From the SBF analysis presented in this paper, we provide not only information about the existence or not of an IGC population, but also an estimate of the slope of the faint end of $n(m)$.

2. Observations and data reduction

Observations of the 16 giant elliptical galaxies and the 4 “blank” regions studied in this paper were done on 2000 April 25 and 27, with the 2.5 m Isaac Newton Telescope (INT) at the Roque de los Muchachos Observatory (La Palma), using the Wide Field Camera and the Sloan R Filter. This work is based on the results obtained by Marín-Franch & Aparicio (2002), where the observations, photometric calibration and data reduction procedures are described in detail, as well as the SBF analysis. We provide here only a short outline of the latter.

The concept of SBF was introduced by Tonry & Schneider (1988), who noted that, in the surface photometry of a galaxy too far to be resolved, a pixel-to-pixel fluctuation is observed due to the Poisson statistics of the spatial distribution of stars, GCs, background galaxies, etc. The variance of the fluctuation depends on the stellar population, the GCS, background galaxies, foreground stars, and, of course, the distance. It can be assumed that the total pixel-to-pixel variance of an image is the sum of all the independent contributions.

The SBF technique involves spectral analysis of the signal and provides as a result the total PSF-convolved variance (P_0), produced by all objects whose spatial flux distribution is convolved with the PSF:

$$P_0 = \sigma_{\text{sp}}^2 + \sigma_{\text{GC}}^2 + \sigma_{\text{BG}}^2 + \sigma_{\text{fs}}^2, \quad (1)$$

where σ_{sp}^2 , σ_{GC}^2 , σ_{BG}^2 , and σ_{fs}^2 are the variances produced by the stellar populations, GCs, background galaxies, and foreground stars, respectively. If a population of IGCs is being analyzed, σ_{sp}^2 can be neglected, and hence

$$P_0 = \sigma_{\text{IGC}}^2 + \sigma_{\text{BG}}^2 + \sigma_{\text{fs}}^2, \quad (2)$$

where σ_{IGC}^2 is the pixel-to-pixel variance produced by the IGC population where this exists.

The pixel-to-pixel variance produced by a class of object can be evaluated as the second moment of the differential number counts of that object population. In this way, σ_{BG}^2 can be obtained from the background $n(m)$, fitted to the resolved point sources, and σ_{fs}^2 from the predicted star counts, computed making use of a Galaxy model.

Once σ_{BG}^2 and σ_{fs}^2 are estimated and P_0 is measured, σ_{IGC}^2 can be easily obtained from equation 2. Note that in Coma, GCs cannot be directly resolved from ground-based observations (except the brightest individuals), so, in order to determine the surface number density of IGCs, SBF analysis becomes necessary.

The surface number density of IGCs (N_{IGC}) can be estimated from σ_{IGC}^2 assuming a fixed GC luminosity function (φ). A fixed φ provides a fixed $\sigma_{\text{IGC}}^2/N_{\text{IGC}}$ ratio that can be

used to transform variances into surface densities. This ratio depends on the photometric calibration.

Marín-Franch & Aparicio’s (2002) results used here are listed in Table 2. The name of the region studied is listed in column 1. In column 2, the distance to the Coma galaxy cluster center is also shown. Finally, the obtained P_0 in the outer region of each galaxy (the region further away from the galactic center, where galactic GCs no longer exist) and in the “blank” areas are listed in column 3. The following discussion is based on these results.

3. Results

Let us consider regions close to the studied galaxies, but beyond the galactic halos. If IGCs existed then σ_{IGC}^2 would be

$$\sigma_{\text{IGC}}^2 = P_0 - \sigma_{\text{BG}}^2 - \sigma_{\text{fs}}^2. \quad (3)$$

P_0 is measured from SBF analysis. But, in order to obtain N_{IGC} , σ_{BG}^2 and σ_{fs}^2 must be deduced first.

3.1. Contribution of foreground stars

Coma is in a nearly perpendicular direction to the Galactic plane, so the expected number of foreground stars is very low and its contribution to the background variance is negligible when compared with the variance produced by the GCSs of the Coma galaxies (Marín-Franch & Aparicio 2002). But foreground stars can produce a significant contribution to the total variance in intergalactic regions, so they must be considered if the variance produced by IGCs and the faint end of $n(m)$ is to be analyzed.

Bahcall & Soneira (1981) computed the predicted star counts in selected fields and photometric bands using their model for the Galaxy. In particular, they computed the predicted star counts in the northern Galactic pole in the R filter down to magnitude 26.5 (Fig. 1). By computing the second moment of these star counts, σ_{fs}^2 can be obtained for the North Galactic Pole. The result is

$$\sigma_{\text{fs}}^2 = (1.50 \pm 0.15) \times 10^{-4} \left(\frac{e^-}{\text{s} \times \text{pix}} \right)^2. \quad (4)$$

assuming a 10% uncertainty for the star counts model predictions. As Coma is very close to the North Galactic Pole, we adopt this value and assume that it is constant over Coma.

3.2. Faint end of the differential galaxy number counts, $n(m)$

The background galaxy variance, σ_{BG}^2 , has to be obtained from the differential galaxy number counts, $n(m)$. Tyson (1988) obtained a slope of $\gamma = 0.39$ for the faint end of $n(m)$ in filter R . More recently, Steidel & Hamilton (1993) obtained slopes in the range $\gamma = 0.30$ – 0.34 , also in R . Unfortunately, the adopted value of γ has considerable effects in the resulting N_{IGC} . For this reason, we have evaluated N_{IGC} considering three values for the $n(m)$ slope, $\gamma = 0.30$, $\gamma = 0.34$, and $\gamma = 0.39$, and has analyzed the results separately. The corresponding zero points of $n(m)$ have been obtained from fits to the resolved point sources measured by Marín-Franch & Aparicio (2002) in which the slope is a fixed parameter.

As an example, $n(m)$ values are shown in Fig. 2 for the three slopes $\gamma = 0.30$, $\gamma = 0.34$, and $\gamma = 0.39$ overplotted on the resolved point sources in region “Blank 3”. It can be seen that the three values of γ are in principle compatible with the resolved galaxy distribution in this region.

The variance σ_{BG}^2 can be now deduced as the second moment of $n(m)$, and σ_{IGC}^2 can be obtained from equation 3. In Table 2, and for each value of γ , the results associated with each galaxy for σ_{BG}^2 are listed in column 4. The error bars of σ_{BG}^2 have been computed taking into account only the $n(m)$ fitting uncertainty. Note that in Marín-Franch & Aparicio (2002) the error bar of σ_{BG}^2 was determined considering possible variations in the slope of the faint end of the $n(m)$ (from $\gamma = 0.30$ to $\gamma = 0.40$), but in the present study, these possible variations are being considered explicitly by studying the cases $\gamma = 0.30$, 0.34 , and 0.39 separately.

3.3. Intergalactic globular clusters

Equation 3 can now be used to derive σ_{IGC}^2 for each region. The results are given in column 5 of Table 2. The number population of IGC, N_{IGC} , can be estimated from σ_{IGC}^2 using the $\sigma_{\text{IGC}}^2/N_{\text{IGC}}$ ratios listed column 6. These ratios were computed in Marín-Franch & Aparicio (2002). The resulting N_{IGC} is listed in column 7. Note that N_{IGC} is expressed in $\text{IGCs}/(\text{''})^2$, while the rest of columns are expressed in *pixels*. The σ_{IGC}^2 uncertainties have been computed adding in quadrature the uncertainties of P_0 and σ_{BG}^2 . On the other hand, the uncertainties of the ratio $\sigma_{\text{IGC}}^2/N_{\text{IGC}}$ have been neglected. The reason is that φ is assumed to be universal (we assume the same φ parameters adopted in Marín-Franch & Aparicio 2002, $\sigma = 1.40$ and $m_R^0 = 27.42$). In this sense, the uncertainty in the φ parameters would introduce a rescaling factor common to all the results, but the relative errors would not change and the proofs of IGCs detection would remain valid. The origin of the galaxy-to-galaxy variations in the ratio $\sigma_{\text{IGC}}^2/N_{\text{IGC}}$ relies on the differences of the

photometric calibration constants.

The values obtained for N_{IGC} for the field regions associated with the 16 galaxies studied in Marín-Franch & Aparicio (2002) (dots) and for four additional intergalactic field regions (stars) are plotted in Fig. 3 versus the distance R to the Coma galaxy cluster center. Each panel corresponds to a value of γ . Regions associated with galaxies were selected in Marín-Franch & Aparicio (2002) with the aim of sampling the background. They are beyond the GCS of each galaxy and they consequently sample the intergalactic field population. The four intergalactic “blank” regions are far from any galaxy. The fact that the average of N_{IGC} for these regions is the same as for the regions associated with galaxies confirms that the field is really being sampled in both cases.

The most significant characteristic of the plots in Fig. 3 is the flat distributions of values. The only point perhaps departing from this trend is that associated with the central galaxy, NGC 4874. Furthermore, it can be seen that N_{IGC} is negative in almost all cases for $\gamma = 0.39$, indicating that this value is unlikely. On the other hand, if $\gamma = 0.30$, then N_{IGC} is clearly a positive number, implying that an IGC population should exist. This population is also detected if $\gamma = 0.34$, but less clearly. It should be noted that, if $\gamma = 0.30$ – 0.34 , N_{IGC} does not correlate with R , and hence with the environment, except for the fact that the density associated with the central galaxy is higher. Rather, the IGC population would be uniformly spread all over Coma. We will discuss this issue further in Section 4.

For each value of γ , we have computed the average $\langle N_{\text{IGC}} \rangle$ in Coma using all but the central points. The results are listed in Table 3 and have been plotted in Fig. 3 by dashed lines. Dotted lines show the $1 \sigma_{\text{points}}$ intervals (σ_{points} is the root mean square of the data point distribution). The estimated errors of the mean have also been computed using the usual formula

$$\sigma_{\langle N_{\text{IGC}} \rangle} = \frac{\sigma_{\text{points}}}{\sqrt{N - 1}}, \quad (5)$$

and are the errors quoted in Table 3.

4. Discussion

4.1. The faint end of the differential galaxy number counts, $n(m)$

The extreme cases considered above for the $n(m)$ slope, $\gamma = 0.30$ and $\gamma = 0.39$, characterize two distinct scenarios. We have seen that the latter produces negative N_{IGC} all over Coma, which indicates that $n(m)$ must be shallower.

Let us consider now in more detail the possibility $\gamma = 0.30$. In this case, Fig. 3 shows

that IGCs would exist and would be spread all over Coma. Furthermore, no relation with the distance to the galaxy cluster center is apparent. However, all the GC formation scenarios mentioned in §1 imply that N_{IGC} should follow the galaxy cluster mass distribution. Assuming this and in order to test our results, we will consider three different galaxy cluster simplistic mass distributions, $\rho(R)$, and analyze the expected N_{IGC} distribution for each model.

Makino (1994) has given for Coma a cut-off radius $r_t = 3.5^\circ$, a core radius $r_c = 0.24^\circ$ (i.e. $r_t/r_c = 14.2$) and, using $H_0 = 72 \pm 8 \text{ km s}^{-1} \text{ Mpc}^{-1}$ (Freedman et al. 2001) for the Hubble parameter, a total mass $1.4 \times 10^{15} M_\odot$. This value for the Hubble parameter corresponds to a distance of 97.2 Mpc and to $r_t = 5.9 \text{ Mpc}$ and $r_c = 0.4 \text{ Mpc}$. In this context, the three considered galaxy cluster mass distribution models correspond to a King model, a homogeneous sphere of radius equal to the cut-off radius of Coma ($r_t = 210'$) and a homogeneous sphere of radius equal to twice the cut-off radius of Coma. All them are plotted in the upper panel of Figure 4. All the mass distributions are normalized to a total galaxy cluster mass of $1.4 \times 10^{15} M_\odot$ (Makino 1994). The vertical solid line represents the Coma cut-off radius, r_t .

Once a mass distribution model is assumed, the expected N_{IGC} can be deduced projecting the galaxy cluster spatial mass distribution and taking into account a GC formation efficiency. The latter is a measure of the fraction of mass converted into GCs. McLaughlin (1999) defined the GC formation efficiency in galaxies as

$$\epsilon_{\text{GC}} = \frac{\rho_{\text{GC}}}{\rho_{\text{gas}} + \rho_{\text{stars}}}, \quad (6)$$

where ρ_{GC} , ρ_{gas} , and ρ_{stars} are the mass densities of GCs, gas, and stars in the galaxy, respectively. McLaughlin (1999) found this definition of ϵ_{GC} to be universal from galaxy to galaxy and equal to 0.0026 ± 0.0005 .

We will use here a similar definition for the intergalactic medium that, for convenience, we define in terms of surface density:

$$\hat{\epsilon}_{\text{IGC}} = \frac{\Sigma_{\text{IGC}}}{\Sigma_{\text{tot}}}. \quad (7)$$

where Σ_{IGC} is the surface mass density of IGCs and Σ_{tot} is the baryonic surface mass density of the galaxy cluster obtained projecting $\rho(R)$.

The relation between the baryonic surface mass density and the IGC surface number density is given by

$$N_{\text{IGC}} = \frac{\hat{\epsilon}_{\text{IGC}} \Sigma_{\text{tot}}}{\langle m \rangle_{\text{GC}}}, \quad (8)$$

where $\langle m \rangle_{\text{GC}}$ is the mean mass of a GC. Assuming $\langle m \rangle_{\text{GC}} = 2.4 \times 10^5$ (McLaughlin 1999), the lower panel of Fig. 4 shows $N_{\text{IGC}}/\hat{\epsilon}_{\text{IGC}}$ as a function of R for the three mass distribution models plotted in the upper panel. This figure shows that the baryonic mass distribution model required to produce an approximately constant, non-null, N_{IGC} distribution along Coma (up to $R \simeq 200'$, at least) should be similar to a very extended homogeneous sphere. The unrealistic nature of this model indicates that a value as low as $\gamma = 0.30$ for the slope of the faint end of $n(m)$ is unlikely. Moreover, it suggests that the IGC surface density, N_{IGC} , is actually zero all over Coma, with the probable exception of the surroundings of the central galaxy. The value of γ that reduces the mean $\langle N_{\text{IGC}} \rangle$ to zero (excluding the central value) can be calculated from interpolation in the data listed in Table 3 and turns out to be $\gamma = 0.36 \pm 0.01$.

The former is the slope of $n(m)$ beyond the detection limit of $R = 23.5$ reached by Tyson (1988) and Steidel & Hamilton (1993) and is valid at least down to the R magnitude significantly contributing to the SBF. This magnitude can be evaluated by considering that in Table 2 the error bars associated with σ_{BG}^2 are, on average, about 5%. If σ_{BG}^2 is computed for different limiting magnitudes, it is found that the variance produced by background galaxies fainter than $m_R = 26.5$ is lower than this value of 5%. The signal produced by fainter galaxies remains below the error bars. In conclusion, $m_R = 26.5$ can be assumed the faintest limit of our determination, so that the slope of the faint end of $n(m)$ is $\gamma = 0.36 \pm 0.01$ (this slope is valid down to $m_R = 26.5$ at least).

For comparison, it is interesting to note that Williams et al. (1996) have measured the slope of $n(m)$ for deeper V and I magnitudes from the Hubble Deep Field. They obtain $\gamma = 0.36$ for V and $\gamma = 0.31$ for I for the magnitude interval [23,26], and $\gamma = 0.17$ for V and $\gamma = 0.18$ for I for the magnitude interval [26,29].

4.2. Intergalactic globular clusters

In §4.1 we concluded that the most likely value for the general IGC density in Coma is zero, and that this is accomplished with a slope $\gamma = 0.36 \pm 0.01$ for the faint end of the background differential galaxy number counts, $n(m)$. We will now further discuss the implications of these results on the IGC population and the overall baryonic mass distribution in Coma.

In Fig. 5, N_{IGC} obtained with $\gamma = 0.36$ is plotted as a function of R , the distance to the Coma center. The points have been computed as an interpolation between the $\gamma = 0.34$ and $\gamma = 0.39$ results listed in Table 2. It can be seen that the mean $\langle N_{\text{IGC}} \rangle$ is zero, as

required. Only NGC 4874 seems to be surrounded by a significant number of IGCs. A King model, such as that plotted in Fig. 4, can now be compared with the IGC distribution. The efficiency $\hat{\epsilon}_{\text{IGC}}$ can be calibrated from the central IGC density $N_{\text{IGC}} = 0.059 \text{ (")}^{-2}$ and is $\hat{\epsilon}_{\text{IGC}} = 7.01 \times 10^{-5}$. Incidentally, this value is two orders of magnitude smaller than that obtained by McLaughlin (1999) for GCs belonging to galaxies.

The former $\hat{\epsilon}_{\text{IGC}}$ and the concentration parameter $r_t/r_c = 14.2$ derived by Makino (1994) for the intergalactic matter in Coma associated with the X-ray radiation can be used to plot the expected distribution of IGCs. The result is shown in Fig. 5, upper panel (solid line). This would be the distribution of IGC in Coma if: (i) the X-ray emission properly samples the baryonic intergalactic mass distribution in Coma; (ii) the GC excess observed in the central region is caused by a genuine IGC population bound by the general Coma potential well, and (iii) if the efficiency $\hat{\epsilon}$ is constant all over Coma. This distribution lies beyond the error bars of several single N_{IGC} values. A higher concentration parameter is required to properly fit the N_{IGC} point distribution. The best fit to a King distribution produces $r_t/r_c = 81.5$ and $\hat{\epsilon}_{\text{IGC}} = 9.5 \times 10^{-5}$. The result has been plotted in the lower panel of Fig. 5.

The reduced chi-square for the best fit results $\chi_\nu^2 = 0.84$ which indicates that the fit is good enough. On the other hand, $\chi_\nu^2 = 3.0$ for the $r_t/r_c = 14.2$ king model fit. For $\nu = 19$ (as in our case), the integral probability of the χ_ν^2 distribution is 0.001 for $\chi_\nu^2 \geq 2.31$, showing that the $r_t/r_c = 14.2$ king model fit can be rejected with a high confidence level.

The concentration parameter $r_t/r_c = 81.5$, implies a core radius of $r_c = 154''$. This is of the order of, or smaller than, the size of the Coma central galaxy NGC 4874. In fact, in Marín-Franch & Aparicio (2002), the spatial structure of the NGC 4874 GCS was studied out to a distance of $161.4''$ from the galaxy center, and its edge was probably not reached. This suggests that the obtained N_{IGC} excess around the center of Coma is produced by the outermost extension of the NGC 4874 primitive GCS rather than being a trace of an IGC system. In other words, the spatial distribution of N_{IGC} shown in Fig. 5 is probably the map of the NGC 4874 GCS.

This result suggests that an IGC population does not exist in Coma. This points toward GCs having been formed only, or almost only, from protogalactic clouds. None of them, or perhaps very few, could have formed in isolated regions. This is in good agreement with the in situ formation scenario for the GCSs (Blakeslee et al. 1997; Forbes, Brodie, & Grillmair 1997; Harris et al. 1998; McLaughlin 1999). If the distribution of IGCs followed the distribution of dark matter in galaxy clusters (Muzzio 1987; West 1993), it would be reasonable to expect that N_{IGC} would show a spatially extended gradient across de galaxy cluster. This not being the case, it seems inappropriate to support the relationship between IGC and dark matter distributions, although it is true that the relationship could still exist

but not be strong enough to be detected.

On the other hand, a number of authors have argued that accretion of IGCs might influence the formation and evolution of galaxies (Muzzio 1987; White 1987; West et al. 1995; Côté et al. 2001). Our results indicate that accretion of IGCs is not a significant effect in galaxy formation and evolutionary processes in the Coma galaxies, since our conclusion is that IGCs do not exist in Coma.

Gurzadyan & Mazure (2001) found the existence of three subgroups of galaxies in Coma, one of them associated with the cD galaxy NGC 4874 and the other two with NGC 4889 and NGC 4839. They conclude that the non-stationarity of the dynamical processes at work in the Coma core is due to the merging of small-scale groups of galaxies. In this context, each subgroup formed separately and then the merger between the different groups took place. In Marín-Franch & Aparicio (2002), five galaxies belonging to the Gurzadyan & Mazure (2001) subgroup 1 (the NGC 4874 group) were analyzed showing that a relation between S_N and the distance to the central galaxy NGC 4874 was compatible with the data. The possibility of accretion of IGCs being responsible for this relation was discussed. In the light of our new results and owing to the absence of IGCs found here, this possibility should be also rejected.

5. Conclusions

The existence of an IGC population in the Coma galaxy cluster has been tested using the SBF. The measured SBF signal is mainly produced by faint galaxies and the IGC population (if it exists). For this reason, the N_{IGC} results reached and the $n(m)$ faint end are connected. As we do not have a precise enough measurement of $n(m)$ in the Coma galaxy cluster, N_{IGC} has been obtained considering three different values for the $n(m)$ slope ($\gamma = 0.30, 0.34,$ and 0.39) and the results have been analyzed separately. The main conclusions of this study are summarized here:

- For the three γ values studied, the results obtained for N_{IGC} have been shown not to correlate with the distance to the central galaxy NGC 4874, and hence with the environment. Comparing the N_{IGC} results obtained for each value of γ with the different Coma galaxy cluster mass distribution model predictions, we suggest that N_{IGC} must be zero all over Coma, with the probably exception of the surroundings of the central galaxy. The most likely $n(m)$ slope that makes $\langle N_{\text{IGC}} \rangle = 0$ is $\gamma = 0.36 \pm 0.01$. This slope has been shown to be valid up to $m_R = 26.5$. For comparison, previous results for the $n(m)$ slope in the R filter range from $\gamma = 0.39$ (Tyson 1988) to $\gamma = 0.31$ – 0.34

(Steidel & Hamilton 1993). This slope has also been measured in the Hubble Deep Field North in the magnitude interval [23,26], resulting in $\gamma = 0.36$ for the V filter and $\gamma = 0.31$ for the I filter (Williams et al. 1996). Our new γ determination falls between previous measurements.

- Our results seem to be in good agreement with the in situ formation for the GCSs (Blakeslee et al. 1997; Forbes, Brodie, & Grillmair 1997; Harris et al. 1998; McLaughlin 1999). The former conclusions point toward GCs having been formed only, or almost only, from protogalactic clouds. None of them, or perhaps very few, could have formed in isolated regions.
- Muzzio (1987) and West (1993) argued that there might exist a relationship between IGC and dark matter distributions. In the light of our results it seems inappropriate to support this idea, although it is true that the relationship could still exist but not be strong enough to be detected.
- Finally, a number of authors have argued that accretion of IGCs might influence the formation and evolution of galaxies (Muzzio 1987; White 1987; West et al. 1995; Côté et al. 2001). Our results suggest that accretion of IGCs might not be a significant effect in galaxy formation and the evolutionary processes in the Coma galaxies since our conclusion is that IGCs do not exist in Coma.

This article is based on observations made with the 2.5 m Isaac Newton Telescope operated on the island of La Palma by the ING in the Spanish Observatorio del Roque de Los Muchachos. This research has been supported by the Instituto de Astrofísica de Canarias (grant P3/94), the DGESIC of the Kingdom of Spain (grant PI97-1438-C02-01), and the DGUI of the autonomous government of the Canary Islands (grant PI1999/008).

REFERENCES

- Bahcall, J. N., & Soneira, R. M. 1981, *ApJS*, 47, 357
- Blakeslee, J. P., Tonry, J. L., & Metzger, M. R. 1997, *AJ*, 114, 482
- Côté, P., McLaughlin, D. E., Hanes, D. A., Bridges, T. J., Geisler, D., Merritt, D., Hesser, J. E., Harris, G. L. H., & Lee, M. G. 2001, *ApJ*, 559, 828
- Forbes, D. A., Brodie, J. P., & Grillmair, C. J. 1997, *AJ*, 113, 1652
- Forte, J. C., Martínez, R. E., & Muzzio, J. C. 1982, *AJ*, 87, 1465
- Freedman, W. L., Madore, B. F., Gibson, B. K., Ferrarese, L., Kelson, D. D., Sakai, S., Mould, J. R., Kennicutt, R. C. Jr., Ford, H. C., Graham, J. A., Huchra, J. P., Hughes, S. M. G., Illingworth, G. D., Macri, L. M., Stetson, P. B. 2001, *ApJ*, 553, 47
- Gurzadyan, V. G., & Mazure, A. 2001, *New Astronomy*, 6, 43
- Harris, W. E., Harris, G. L. H., & McLaughlin, D. E. 1998, *AJ*, 115, 1801
- King, I. R. 1962, *AJ*, 67, 471
- Makino, N., 1994, *PASJ*, 46, 139
- Marín-Franch, A., & Aparicio, A. 2002, *ApJ*, 568, 174
- McLaughlin, D. E. 1999, *AJ*, 117, 2398
- Muzzio, J. C. 1987, *PASP*, 99, 245
- Steidel, C. C., & Hamilton, D. 1993, *AJ*, 105, 2017
- Tonry, J. L., & Schneider, D. P. 1988, *AJ*, 96, 807
- Tyson, J. A. 1988, *AJ*, 96, 1
- van den Bergh, S. 1956, *PASP*, 68, 449
- van den Bergh, S. 1958, *The Observatory*, 78, 85
- West, M. J. 1993, *MNRAS*, 265, 755
- West, M. J., Côté, P., Jones, C., Forman, W., & Marzke, R. O. 1995, *ApJ*, 453, L77
- White, R. E. 1987, *MNRAS*, 227, 185

Williams, R. E. et al., 1996, AJ, 112, 1335

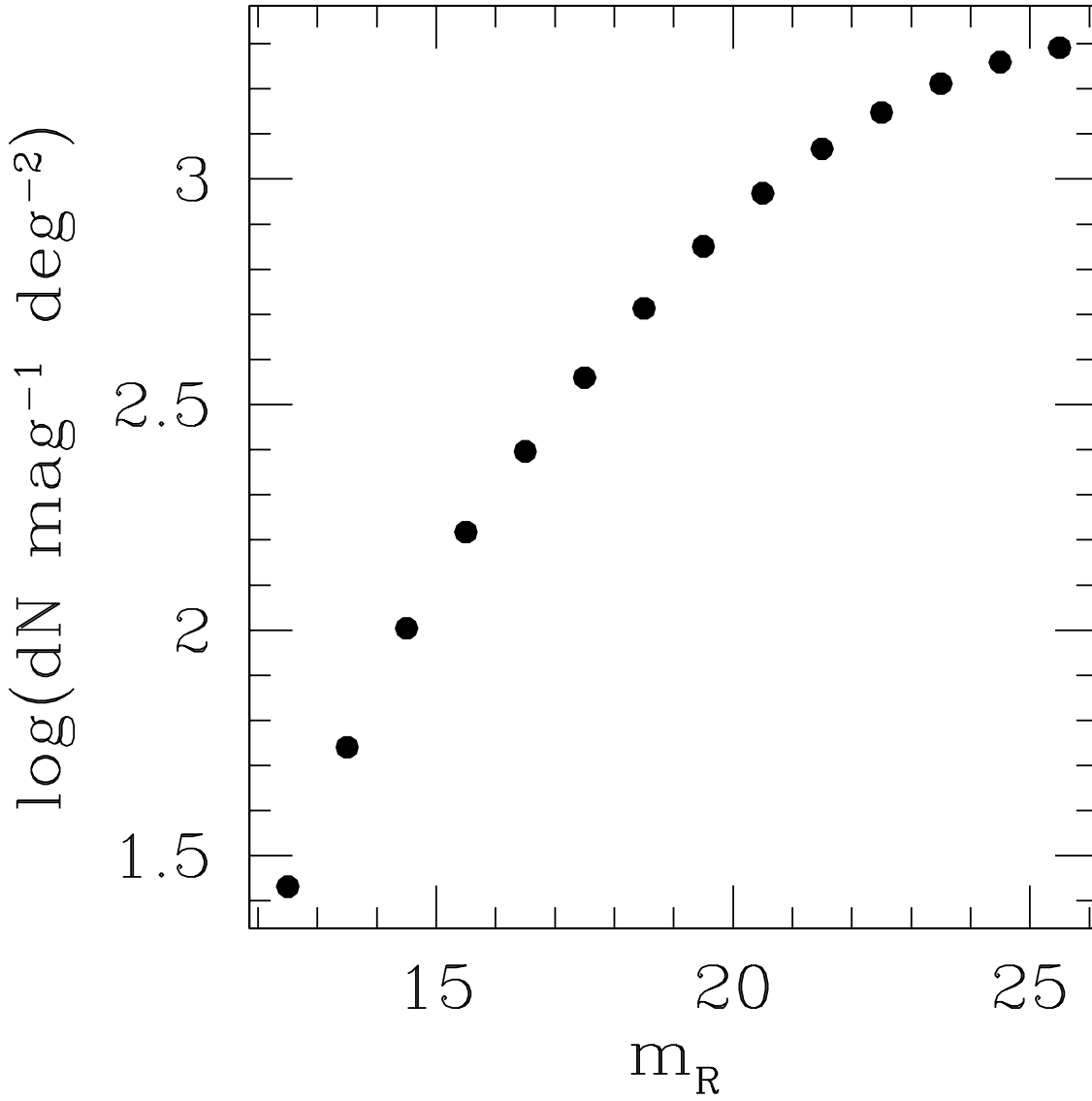


Fig. 1.— Star counts predicted by the Bahcall-Soneira Galaxy model in the direction of the North Galactic Pole (Bahcall & Soneira 1981).

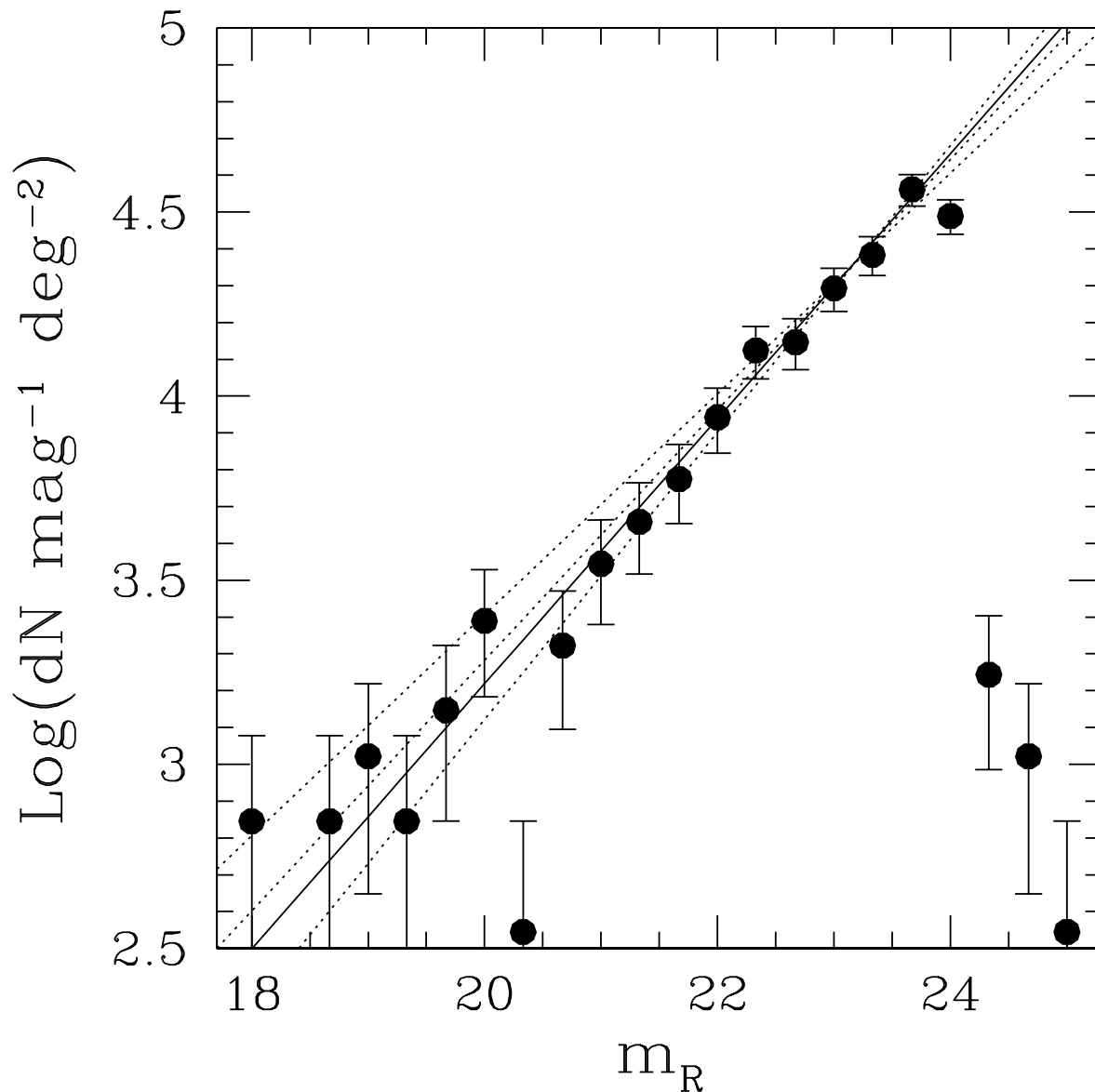


Fig. 2.— Background differential galaxy number counts, $n(m)$, fitted to resolved point source distribution in the region “Blank 3”. The fit has been performed using the three values for the $n(m)$ slope $\gamma = 0.30, 0.34,$ and 0.39 discussed in the text as fixed parameters. The error bars represent the Poissonian error of the detection counts. Solid line represents the obtained $n(m)$ in this paper (see §4.1).

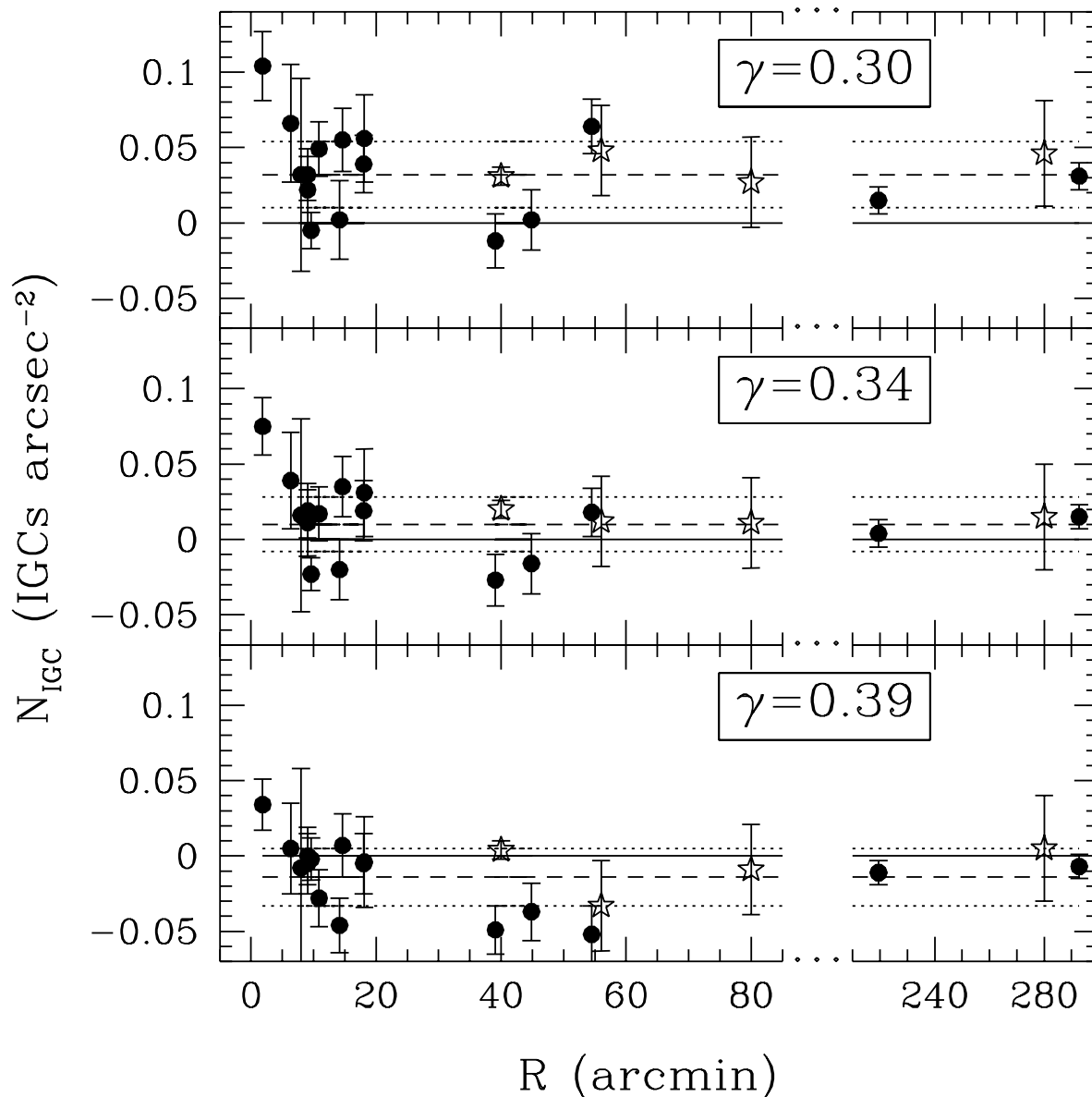


Fig. 3.— The IGC population in Coma plotted for three possible values of the $n(m)$ slope, γ . Horizontal axis represents the distance to the Coma galaxy cluster center, and vertical axis represents the IGCs surface number density. Full lines indicate the zero density level. Dashed lines represent the mean for each case while dotted lines show the $\pm 1\sigma$ of the mean. Full circles represent the outskirts of the 16 galaxies studied, while open stars represent the four control fields. See text for details.

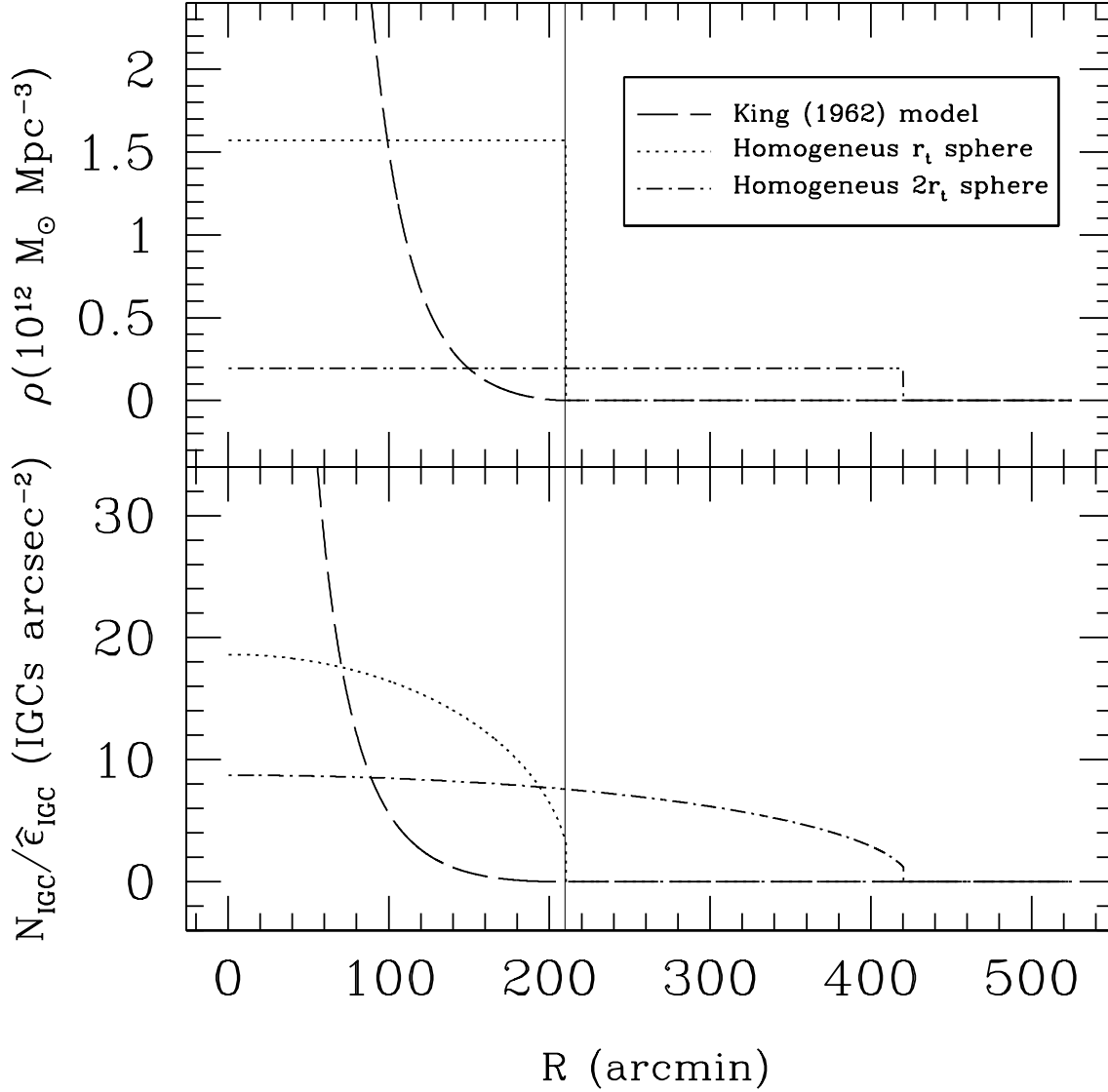


Fig. 4.— Upper panel: The total mass density (ρ) is plotted as a function of the distance to the galaxy cluster center (R) for three different galaxy cluster mass density distributions; King (1962) model (long dash), homogeneous sphere of radius equal to the Coma radius (dots) and homogeneous sphere of radius twice the Coma radius (short dash). Lower panel: IGC surface number density normalized to the globular cluster formation efficiency ($N_{\text{IGC}}/\hat{\epsilon}_{\text{IGC}}$) for each of the former mass distributions. See text for details.

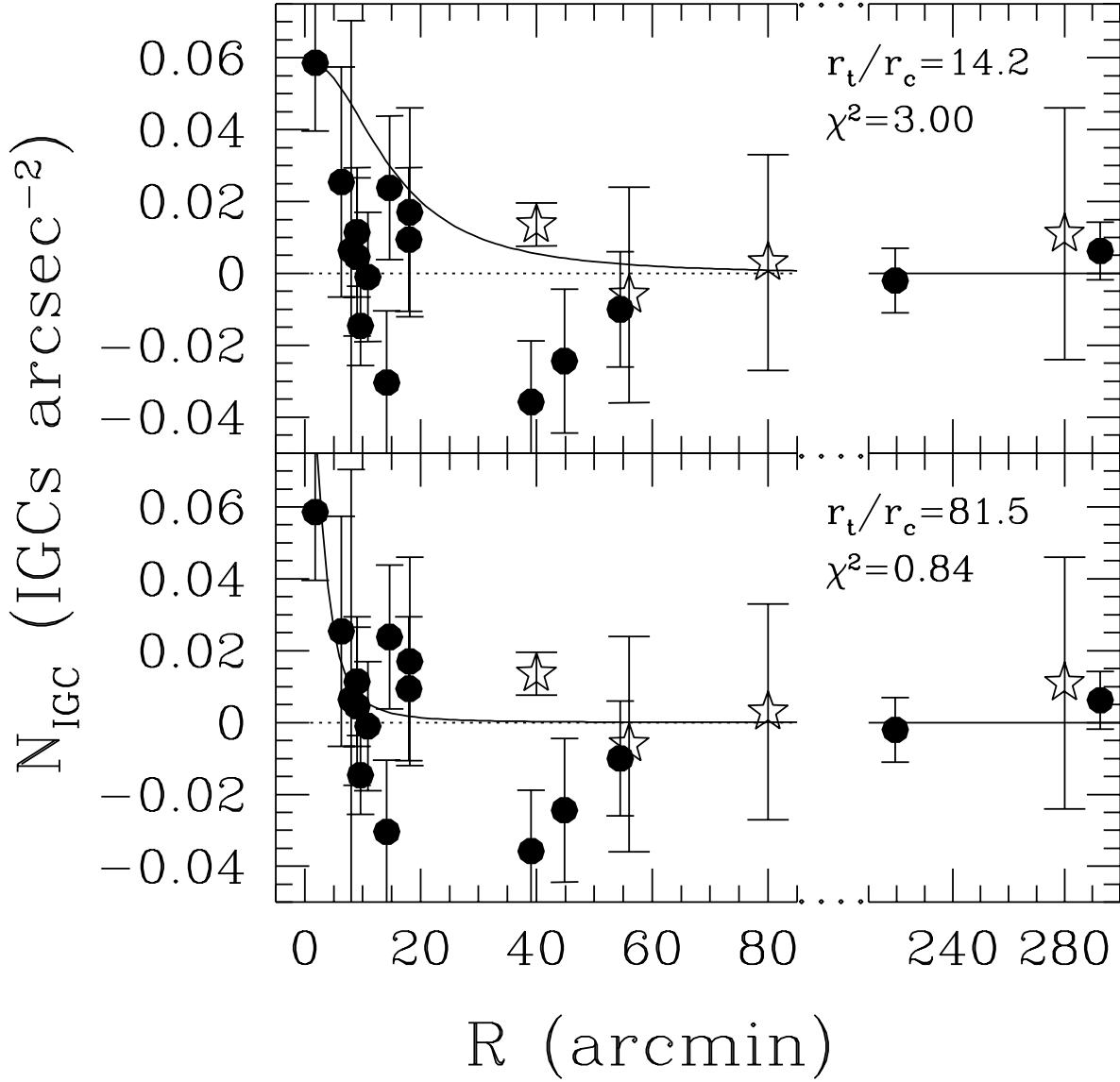


Fig. 5.— N_{IGC} interpolated for the resulting case $\gamma = 0.36$. Upper panel: The theoretical expectation from the King (1962) model has been fitted to our central N_{IGC} result considering the Makino (1994) core radius (solid line); Lower panel: N_{IGC} results have been fitted with a King (1962) model considering r_t/r_c and $\hat{\epsilon}_{\text{IGC}}$ as free parameters. The best fit is plotted with a solid line.

Table 1. Notation summary.

Globular Cluster	GC
Intergalactic Globular Cluster	IGC
Globular Cluster System	GCS
Surface Brightness Fluctuations	SBF
Differential Galaxy Number Counts	$n(m)$
Differential Galaxy Number Counts Slope	γ
Globular Cluster Luminosity Function	φ

Table 2. IGCs in the environments of the 16 Coma galaxies^(a)

Galaxy	R ($'$)	F_0 $10^{-4} \times \left(\frac{e^-}{s \times \text{pix}}\right)^2$	σ_{BG}^2 $10^{-4} \times \left(\frac{e^-}{s \times \text{pix}}\right)^2$	σ_{IGC}^2 $10^{-4} \times \left(\frac{e^-}{s \times \text{pix}}\right)^2$	$\sigma_{\text{IGC}}^2/N_{\text{IGC}}^{(b)}$	N_{IGC} IGCs/ $('')^2$
$\gamma = 0.30$						
NGC 4874	0	31.8 ± 1.2	22.6 ± 1.2	7.7 ± 1.7	0.067	0.104 ± 0.023
NGC 4889	8.05	26.2 ± 2.1	19.8 ± 1.4	4.9 ± 2.9	0.067	0.066 ± 0.039
IC 4012	10.68	18.0 ± 1.1	14.9 ± 1.2	1.6 ± 1.6	0.067	0.022 ± 0.022
IC 4021	10.88	16.4 ± 1.0	12.5 ± 0.8	2.4 ± 1.3	0.067	0.032 ± 0.017
IC 4026	12.62	17.2 ± 1.1	12.0 ± 0.9	3.7 ± 1.4	0.067	0.049 ± 0.018
IC 4041	16.38	21.2 ± 1.1	15.6 ± 1.1	4.1 ± 1.6	0.067	0.055 ± 0.021
IC 4045	19.85	19.7 ± 1.1	15.3 ± 0.9	2.9 ± 1.4	0.067	0.039 ± 0.019
IC 4051	19.95	26.1 ± 2.1	20.4 ± 0.8	4.2 ± 2.2	0.067	0.056 ± 0.029
IC 3976	6.78	11.5 ± 3.0	8.4 ± 1.3	1.6 ± 3.2	0.045	0.032 ± 0.064
IC 3959	12.67	15.2 ± 1.0	13.6 ± 0.8	0.1 ± 1.3	0.059	0.002 ± 0.026
MCG +5 -31 -063	8.93	13.5 ± 0.6	12.3 ± 0.3	-0.3 ± 0.7	0.059	-0.005 ± 0.012
NGC 4839	43.12	10.3 ± 1.0	8.7 ± 0.1	0.1 ± 1.0	0.046	0.002 ± 0.020
NGC 4840	37.43	9.5 ± 0.8	8.6 ± 0.3	-0.6 ± 0.9	0.046	-0.012 ± 0.018
NGC 4816	52.60	16.5 ± 1.1	10.8 ± 0.4	4.2 ± 1.2	0.060	0.064 ± 0.018
NGC 4673	217.07	15.5 ± 0.6	12.9 ± 0.4	1.1 ± 0.7	0.067	0.015 ± 0.009
IC 3651	290.32	16.7 ± 0.6	12.9 ± 0.3	2.3 ± 0.7	0.067	0.031 ± 0.009
Blank 1	40	10.3 ± 0.3	6.7 ± 0.4	2.1 ± 0.5	0.060	0.031 ± 0.007
Blank 2	56	14.5 ± 2.0	9.8 ± 0.3	3.2 ± 2.0	0.060	0.048 ± 0.030
Blank 3	80	11.0 ± 2.0	7.7 ± 0.3	1.8 ± 2.0	0.060	0.027 ± 0.030
Blank 4	280	16.0 ± 3.0	11.4 ± 0.5	3.1 ± 3.0	0.060	0.046 ± 0.044
$\gamma = 0.34$						
NGC 4874	0	31.8 ± 1.2	24.7 ± 0.8	5.6 ± 1.4	0.067	0.075 ± 0.019
NGC 4889	8.05	26.2 ± 2.1	21.8 ± 1.2	2.9 ± 2.4	0.067	0.039 ± 0.032
IC 4012	10.68	18.0 ± 1.1	15.7 ± 1.2	0.8 ± 1.6	0.067	0.011 ± 0.022
IC 4021	10.88	16.4 ± 1.0	13.5 ± 0.9	1.4 ± 1.3	0.067	0.019 ± 0.018
IC 4026	12.62	17.2 ± 1.1	14.4 ± 0.9	1.3 ± 1.4	0.067	0.017 ± 0.018
IC 4041	16.38	21.2 ± 1.1	17.1 ± 1.0	2.6 ± 1.5	0.067	0.035 ± 0.020
IC 4045	19.85	19.7 ± 1.1	16.8 ± 1.0	1.4 ± 1.5	0.067	0.019 ± 0.020
IC 4051	19.95	26.1 ± 2.1	22.3 ± 0.8	2.3 ± 2.2	0.067	0.031 ± 0.029
IC 3976	6.78	11.5 ± 3.0	9.2 ± 1.3	0.8 ± 3.2	0.045	0.016 ± 0.064
IC 3959	12.67	15.2 ± 1.0	15.0 ± 0.8	-1.3 ± 1.3	0.059	-0.020 ± 0.020
MCG +5 -31 -063	8.93	13.5 ± 0.6	13.4 ± 0.3	-1.5 ± 0.7	0.059	-0.023 ± 0.011
NGC 4839	43.12	10.3 ± 1.0	9.6 ± 0.1	-0.8 ± 1.0	0.046	-0.016 ± 0.020
NGC 4840	37.43	9.5 ± 0.8	9.4 ± 0.3	-1.4 ± 0.9	0.046	-0.027 ± 0.017
NGC 4816	52.60	16.5 ± 1.1	13.8 ± 0.3	1.2 ± 1.1	0.060	0.018 ± 0.016
NGC 4673	217.07	15.5 ± 0.6	13.7 ± 0.3	0.3 ± 0.7	0.067	0.004 ± 0.009
IC 3651	290.32	16.7 ± 0.6	14.1 ± 0.2	1.1 ± 0.6	0.067	0.015 ± 0.008
Blank 1	40	10.3 ± 0.3	7.4 ± 0.4	1.4 ± 0.5	0.060	0.021 ± 0.007
Blank 2	56	14.5 ± 2.0	12.2 ± 0.3	0.8 ± 2.0	0.060	0.012 ± 0.030
Blank 3	80	11.0 ± 2.0	8.7 ± 0.3	0.8 ± 2.0	0.060	0.012 ± 0.030
Blank 4	280	16.0 ± 3.0	12.5 ± 0.5	1.0 ± 3.0	0.060	0.015 ± 0.045
$\gamma = 0.39$						
NGC 4874	0	31.8 ± 1.2	27.7 ± 0.6	2.6 ± 1.3	0.067	0.034 ± 0.017
NGC 4889	8.05	26.2 ± 2.1	24.3 ± 1.2	0.4 ± 2.4	0.067	0.005 ± 0.030
IC 4012	10.68	18.0 ± 1.1	16.9 ± 1.2	-0.4 ± 1.6	0.067	-0.005 ± 0.020
IC 4021	10.88	16.4 ± 1.0	14.9 ± 1.1	0.0 ± 1.5	0.067	0.000 ± 0.019
IC 4026	12.62	17.2 ± 1.1	17.8 ± 0.9	-2.1 ± 1.4	0.067	-0.028 ± 0.019

Table 2—Continued

Galaxy	R ($'$)	P_0 $10^{-4} \times \left(\frac{e^-}{s \times \text{pix}}\right)^2$	σ_{BG}^2 $10^{-4} \times \left(\frac{e^-}{s \times \text{pix}}\right)^2$	σ_{IGC}^2 $10^{-4} \times \left(\frac{e^-}{s \times \text{pix}}\right)^2$	$\sigma_{\text{IGC}}^2/N_{\text{IGC}}^{(b)}$	N_{IGC} IGCs/ $('')^2$
IC 4041	16.38	21.2 ± 1.1	19.2 ± 1.0	0.5 ± 1.5	0.067	0.007 ± 0.021
IC 4045	19.85	19.7 ± 1.1	18.6 ± 1.2	-0.4 ± 1.6	0.067	-0.005 ± 0.020
IC 4051	19.95	26.1 ± 2.1	24.9 ± 0.9	-0.3 ± 2.3	0.067	-0.004 ± 0.030
IC 3976	6.78	11.5 ± 3.0	10.3 ± 1.4	-0.4 ± 3.3	0.045	-0.008 ± 0.066
IC 3959	12.67	15.2 ± 1.0	16.7 ± 0.7	-3.0 ± 1.2	0.059	-0.046 ± 0.018
MCG +5 -31 -063	8.93	13.5 ± 0.6	12.1 ± 0.3	-0.1 ± 0.7	0.059	-0.002 ± 0.014
NGC 4839	43.12	10.3 ± 1.0	10.7 ± 0.1	-1.9 ± 1.0	0.046	-0.037 ± 0.019
NGC 4840	37.43	9.5 ± 0.8	10.5 ± 0.2	-2.5 ± 0.8	0.046	-0.049 ± 0.016
NGC 4816	52.60	16.5 ± 1.1	18.5 ± 0.6	-3.5 ± 1.3	0.060	-0.052 ± 0.019
NGC 4673	217.07	15.5 ± 0.6	14.8 ± 0.2	-0.8 ± 0.6	0.067	-0.011 ± 0.008
IC 3651	290.32	16.7 ± 0.6	15.7 ± 0.2	-0.5 ± 0.6	0.067	-0.007 ± 0.008
Blank 1	40	10.3 ± 0.3	8.5 ± 0.4	0.3 ± 0.5	0.060	0.004 ± 0.006
Blank 2	56	14.5 ± 2.0	15.2 ± 0.3	-2.2 ± 2.0	0.060	-0.033 ± 0.030
Blank 3	80	11.0 ± 2.0	10.1 ± 0.3	-0.6 ± 2.0	0.060	-0.009 ± 0.030
Blank 4	280	16.0 ± 3.0	14.1 ± 0.5	0.4 ± 3.0	0.060	0.006 ± 0.045

^(a)Columns P_0 , σ_{BG}^2 and $\sigma_{\text{IGC}}^2/N_{\text{IGC}}$ have been extracted from the analysis done in Marín-Franch & Aparicio (2002). $1 \text{ pix} = 0.333''$.

^(b)Theoretical value based on the assumption that the φ is universal with $\sigma = 1.40$ and $m_R^0 = 27.42$. This value depends on the photometric calibration.

Table 3. Mean surface number density of IGCs in Coma.

γ	$\langle N_{\text{IGC}} \rangle$ (IGCs/('') ²)
0.30	0.032 ± 0.005
0.34	0.010 ± 0.004
0.39	-0.014 ± 0.004